

Incipient modulated phase in $\text{Sr}_{1-x}\text{Ca}_x\text{TiO}_3$

Benoît Fauqué¹, Daniel A. Chaney², Philippe Bourges³, Stéphane Raymond⁴, Arno Hiess^{5,6}, Paul Steffens⁵, Benoît Baptiste⁷, Luigi Paolasini², Alexeï Bosak², Kamran Behnia¹, and Yasuhide Tomioka⁸

¹ Laboratoire de Physique et d'Etude de Matériaux (CNRS)

ESPCI Paris, Université PSL, 75005 Paris,

France ² European Synchrotron Radiation Facility,

71 avenue des Martyrs, 38000 Grenoble, France

³ Laboratoire Léon Brillouin,

CEA-CNRS, Université Paris-Saclay,

CEA Saclay, 91191 Gif-sur-Yvette, France

⁴ Univ. Grenoble Alpes, CEA, IRIG,

MEM, MDN, 38000 Grenoble, France

⁵ Institut Laue-Langevin, 71 Avenue des Martyrs,

38042 Grenoble Cedex 9, France

⁶ European Spallation Source ERIC,

P.O. Box 176, 22100 Lund,

Sweden ⁷ IMPMC-Sorbonne Université and CNRS,

4, place Jussieu, 75005 Paris, France

⁸ National Institute of Advanced Industrial Science and Technology (AIST),

Tsukuba, 305-8565, Japan

(Dated: January 16, 2026)

Nanometer-scale modulations can spontaneously emerge in complex materials when multiple degrees of freedom interact. Here we demonstrate that ferroelectric $\text{Sr}_{1-x}\text{Ca}_x\text{TiO}_3$ lies in close proximity to an incipient structurally modulated phase. Using inelastic neutron and X-ray scattering, we show that upon cooling, dipolar fluctuations strongly couple to and soften the c_{44} transverse acoustic mode. We identify the wavevector at which this softening is maximal, thereby defining the characteristic length scale of the modulation. Calcium substitution enhances both the amplitude and the wavevector of the softening by strengthening the ferroelectric and antiferrodistortive instabilities. Our results demonstrate that nonlinear flexoelectric phonon coupling tends to stabilize a modulated state that cooperates with, rather than competes against, the other lattice instabilities in SrTiO_3 .

Competing interactions may lead to modulated phases in condensed matter, characterized by periodic spatial variations of the relevant order parameter [1]. The modulation period is set by the relative strengths of the active degrees of freedom and can be tuned by temperature or external fields. Such states, found in manganites [2, 3], high-temperature cuprates [4], and two-dimensional electron gases under strong magnetic fields [5], give rise to rich phase diagrams and novel functionalities. Understanding how these modulated phases interact with other lattice or electronic instabilities is therefore crucial for both fundamental insight and materials design. Recently, SrTiO_3 has been identified as a new member of this class of nanoscale-modulated materials [6–10].

SrTiO_3 is a paradigmatic system for exploring novel structural and electronic phases [11, 12], largely due to its proximity to multiple lattice instabilities. Two are well-established: the anti-ferro-distortive (AFD) transition, where TiO_6 octahedra rotate in an anti-phase manner (Fig. 1a), and the quantum-paraelectric regime, where dipolar fluctuations grow upon cooling yet never condense into long-range ferroelectric order [13].

Despite decades of study, the quantum-paraelectric phase of SrTiO_3 remains unsettled. It has been described either as an incipient ferroelectric state suppressed by zero-point fluctuations [13–16], or as a regime where the soft transverse-optical (TO) mode hybridizes with an acoustic branch [17–20]. Coupling between the TO mode and the transverse-acoustic (TA) c_{44} branch has been documented for decades [21–27], but only recently did Fauqué *et al.* [6] show that the TA softening is strongly wavevector-dependent, with a pronounced anomaly along the (110) direction at $Q_{\min} \simeq 0.02$ (r.l.u.), sketched on (Fig. 1c). This identifies a modulated state in which polarization fluctuations are accompanied by a transverse strain modulation with a characteristic wavelength of ~ 15 nm (Fig. 1f). Recent complementary observations have reinforced this picture including ultrafast X-ray diffraction revealing this polar-acoustic collective mode [8] and STEM imaging of fluctuating polar nanoscale domains displaying similar length scales [9].

This nanoscale modulation is governed purely by lattice degrees of freedom and nonlinear phonon interactions. Within Landau–Ginzburg–Devonshire (LGD) theory [7, 30], such a state can emerge at the mean-field level when the softening TO mode approaches the TA branch. The flexoelectric coupling, which links polariza-

* benoit.fauque@espci.fr

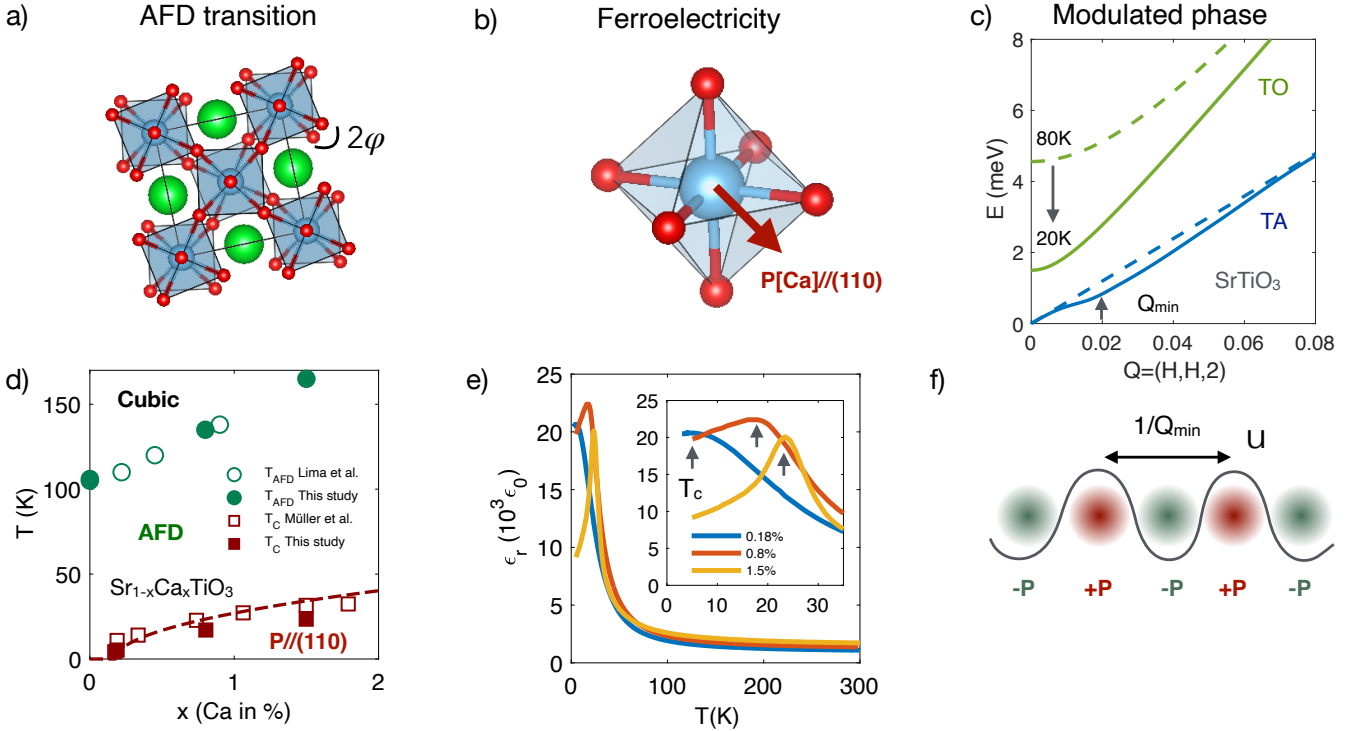


Figure 1. Lattice instabilities in $\text{Sr}_{1-x}\text{Ca}_x\text{TiO}_3$ (a) Antiferrodistortive (AFD) transition at T_{AFD} . (b) Polar distortion: Ca^{2+} substitution stabilizes ferroelectricity along the [110] direction. (c) Schematic of TO-TA coupling in $\text{Sr}_{1-x}\text{Ca}_x\text{TiO}_3$: softening of the transverse-optical (TO) mode induces a concomitant softening of the transverse-acoustic (TA, c_{44}) branch, which is maximal at Q_{min} , signaling a tendency toward a modulated phase. (d) Phase diagram of $\text{Sr}_{1-x}\text{Ca}_x\text{TiO}_3$: T_{AFD} and Curie temperature T_C as a function of Ca concentration, compared with previous studies [28, 29]. (e) Dielectric constant as a function of temperature for three Ca concentrations; the inset highlights the low-temperature region below 35 K. (f) Real-space illustration of TO-TA coupling: dipolar fluctuations are accompanied by a transverse strain modulation with wavelength $\sim 1/Q_{\text{min}} \simeq 15 \text{ nm}$ in pristine SrTiO_3 .

tion to strain gradients, can drive the TA mode unstable at a finite wavevector and, if sufficiently strong, stabilize a static incommensurate structure [30]. However, once thermal and quantum fluctuations are included this ordered state becomes fragile, giving way to a competition between homogeneous ferroelectricity and a melted, fluctuating version of the modulated phase [7].

Here we show that, in $\text{Sr}_{1-x}\text{Ca}_x\text{TiO}_3$, the melted modulated phase does not compete with ferroelectricity but instead reinforces it. Both the magnitude and the characteristic wavevector of the TA softening increase with Ca substitution, which simultaneously enhances the ferroelectric and AFD instabilities. At the highest dopings, the TA branch develops a waterfall-like dispersion that lies beyond the mean-field flexoelectric theory. Together, these results demonstrate that SrTiO_3 hosts an incipient modulated phase that is intrinsically intertwined with its other lattice instabilities, providing a microscopic foundation for its nanoscale structural modulation.

Figure 1d presents the phase diagram of $\text{Sr}_{1-x}\text{Ca}_x\text{TiO}_3$, showing the evolution of the ferroelectric (T_C , red) and antiferrodistortive (T_{AFD} , green)

transitions with Ca substitution. Both T_C [29] and T_{AFD} [28] increase as Ca content rises. The temperature dependence of the dielectric constant for three single crystals ($x = 0.18\%$, 0.8% , 1.5%) is shown in Fig. 1e, confirming that ferroelectricity emerges above a critical Ca concentration $x_c \simeq 0.18\%$ [29] along the (110) direction (Fig. 1b). Sample preparation and characterization details are provided in [31].

The low-energy phonon spectrum was measured using the cold triple-axis spectrometers IN12 and THALES at the Institut Laue-Langevin, Grenoble, with samples mounted in the (H,H,L) scattering plane in the (002) Brillouin zone. High-resolution configurations probed the transverse acoustic (TA) c_{44} branch near the Bragg peak, while standard settings accessed larger wavevectors ($H \gtrsim 0.03$). Complementary inelastic X-ray scattering (IXS) measurements were performed on ID28 at ESRF. Experimental details and data analysis procedures are given in Sections B and C of [31].

Figure 2a,b show energy scans for the 1.5% Ca-doped sample at $\mathbf{Q} = (H, H, 2)$, taken for $H = 0.017$ to 0.035 at 150 K and 20 K, respectively. At high temperature, the

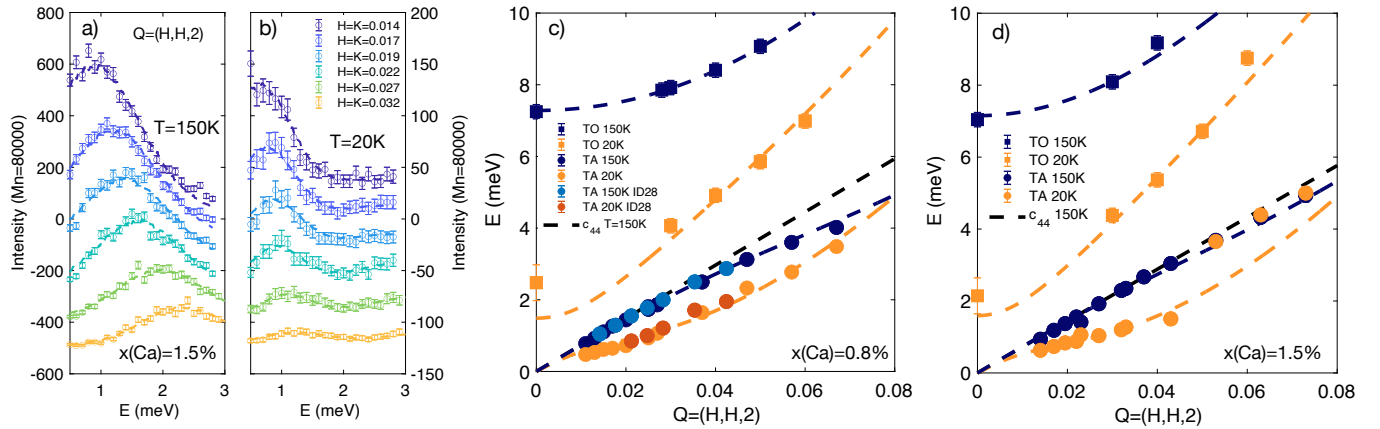


Figure 2. TA softening in $\text{Sr}_{1-x}\text{Ca}_x\text{TiO}_3$: (a–b) Energy scans at $\mathbf{Q} = (H, H, 2)$ for $H = K = 0.014\text{--}0.032$ at (a) $T = 150$ K and (b) $T = 20$ K for $x = 1.5\%$. Fits including a convolution with the experimental resolution are shown in dotted lines (see [31]). (c) Dispersion of the TO (squares) and TA (circles) modes for $x = 0.8\%$ at $T = 150$ K (dark blue: INS; light blue: IXS) and $T = 20$ K (orange: INS; red: IXS). (d) Same as (c) for $x = 1.5\%$. Both dispersions are fitted using the mean-field Landau-Ginzburg-Devonshire solution [30] (see text). At the highest doping, the model fails to capture the abrupt change of the TA dispersion around $H = K = 0.04$.

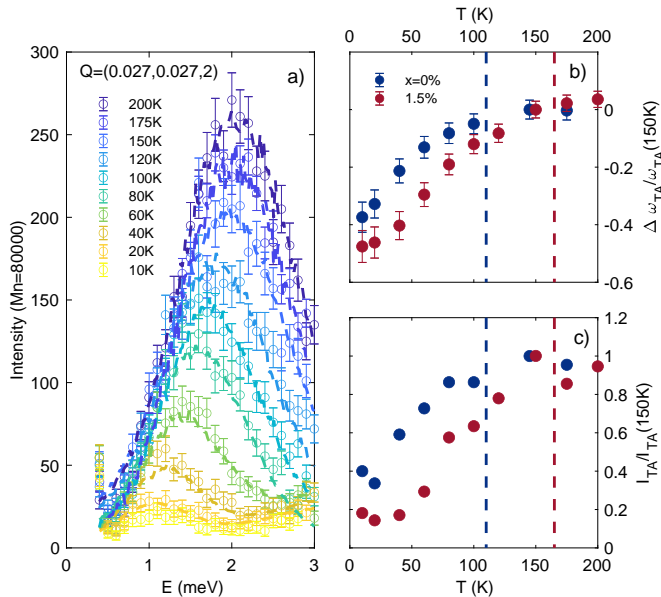


Figure 3. Temperature dependence of the TA softening in $\text{Sr}_{1-x}\text{Ca}_x\text{TiO}_3$: Energy scans at $\mathbf{Q} = (0.027, 0.027, 2)$ in the Ca-doped sample ($x = 1.5\%$) from $T = 10\text{--}200$ K (high-resolution mode). Fits including a convolution with the experimental resolution are shown in dotted lines (see [31]). (b–c) Temperature dependence of the TA mode: (b) energy and (c) intensity for $x=0$ (dark blue) at $H=K=0.017$ and 1.5% (dark red) at $H=K=0.027$. The dashed vertical line indicates the structural transition T_{AFD} . The TA mode softening begins below T_{AFD} .

TA mode energy increases with H , while at low temperature the mode remains nearly constant across the same momentum range, revealing a pronounced softening. To

extract quantitative dispersions, the energy scans were fitted with a damped harmonic oscillator (DHO) model convolved with the experimental resolution (see [31]). The resulting TO and TA dispersions for $x = 0.8\%$ and $x = 1.5\%$ are shown in Fig. 2c,d. At 150 K, the TA mode exhibits a quasi-linear dispersion, in agreement with the c_{44} elastic constant measured by ultrasound [32]. At low temperatures, the TA mode deviates strongly from linearity, forming a plateau at $H = 0.025$ for $x = 0.8\%$ and at $H \approx 0.035$ for $x = 1.5\%$. At the highest doping, the dispersion shows a step-like behavior, reminiscent of the "waterfall" dispersion observed in the TO mode of relaxor perovskites [33–35].

The temperature dependence of the TA mode at $H \approx 0.027$ is shown in Fig. 3. Upon cooling, the mode softens by roughly 50%, accompanied by a sixfold decrease in intensity. The softening commences just below the AFD transition ($T_{\text{AFD}} \simeq 165$ K at $x = 1.5\%$), in agreement with previous studies of pure SrTiO_3 [6].

Independent confirmation of the presence of the TA softening across multiple Brillouin zones is provided by IXS measurements for $x = 0.8\%$, performed around $\mathbf{Q} = (4, 4, 0)$. Despite differences in energy resolution (IXS ~ 1.5 meV vs. INS ~ 0.4 meV) and Q -space coverage, the extracted dispersions are in excellent agreement, as shown in Fig. 2c, confirming the robustness of the neutron results. We note that INS allowed us to probe the TA mode slightly closer to the Bragg peak when compared to IXS. This is likely due to the superior energy resolution of the INS technique.

Our measurements reveal that Ca doping not only steepens the TA softening in $\text{Sr}_{1-x}\text{Ca}_x\text{TiO}_3$ (Fig. 4a–c), but also shifts the minimum to higher Q (Fig. 4d). Even at the highest doping, the softening remains incomplete, and no static incommensurate order is observed (see [31]

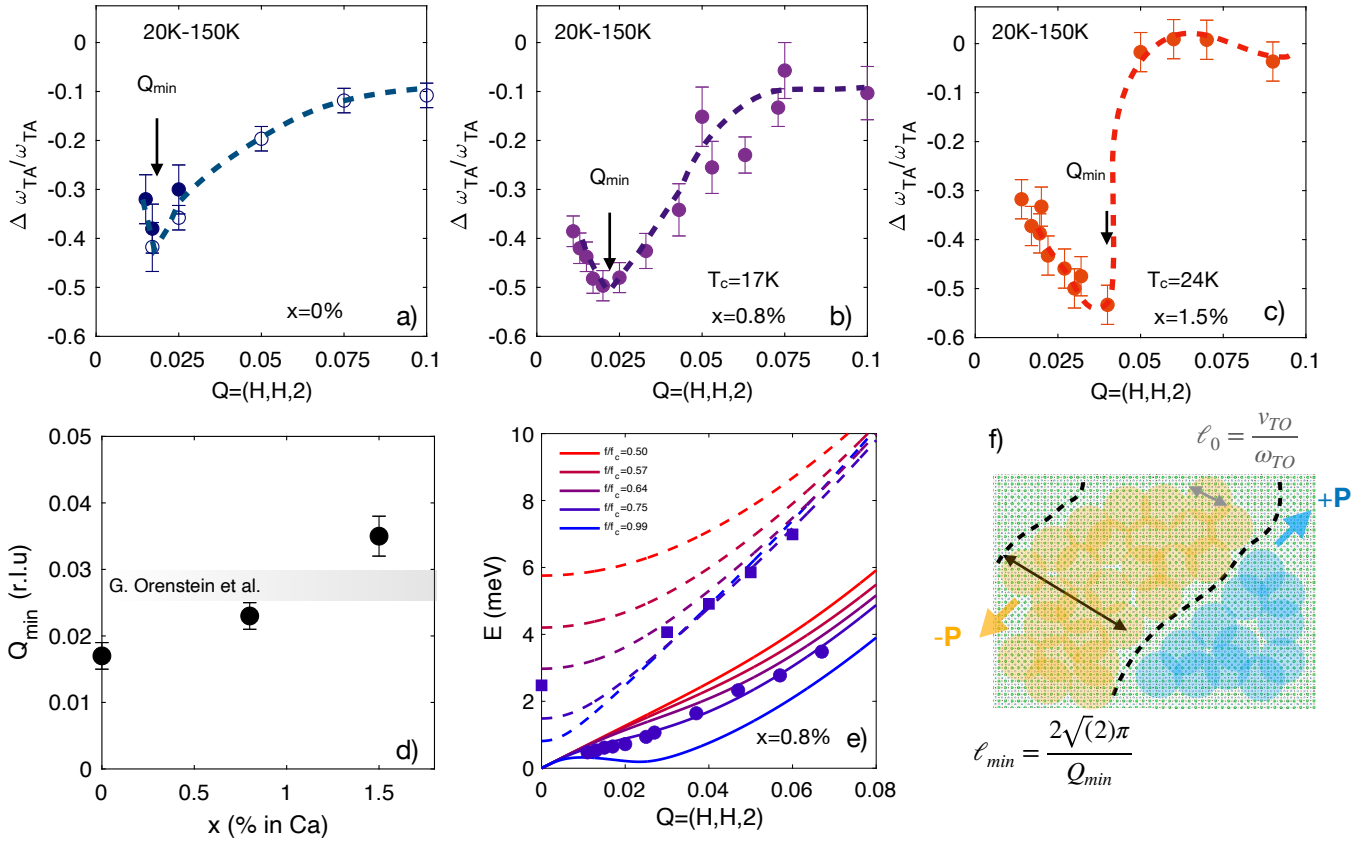


Figure 4. **Doping evolution of the TA softening in $\text{Sr}_{1-x}\text{Ca}_x\text{TiO}_3$:** Q-dependence of the TA softening between 20 K and 150 K, $\frac{\Delta\omega_{TA}}{\omega_{TA}} = [\omega_{TA}(20 \text{ K}) - \omega_{TA}(150 \text{ K})]/\omega_{TA}(150 \text{ K})$, for (a) $x = 0$, (b) $x = 0.8\%$, and (c) $x = 1.5\%$ in $\text{Sr}_{1-x}\text{Ca}_x\text{TiO}_3$. Dashed lines are a guide to the eye. Closed circles are results from this work; open circles are taken from Ref. [6]. (d) Doping evolution of Q_{\min} . The gray band indicates the wavevector where the TO-TA coupling was found to be maximal in Ref. [8]. (e) Dispersion of the TO (dotted lines) and TA (solid lines) modes in the presence of a flexoelectric coupling f [30]. As the TO mode softens, f approaches the critical value f_c , above which an incommensurate phase is stabilized. Closed squares and circles denote the TO and TA modes, respectively, for $x = 0.8\%$. (f) Real-space schematic illustrating the two characteristic length scales in $\text{Sr}_{1-x}\text{Ca}_x\text{TiO}_3$: around a Ca dopant, a ferroelectric moment forms over a length ℓ_0 , which clusters with other dipoles over a longer scale $\ell_{\min} = 2\sqrt{2}\pi/Q_{\min}$.

Section B), indicating that the system develops a dynamically modulated lattice instability rather than a static modulation. Remarkably, the Q_{\min} in doped samples coincides with the wavevector of maximal TO-TA coupling under terahertz excitation in pure SrTiO_3 [8], suggesting that ferroelectricity, whether induced by doping or light [36–38], shifts Q_{\min} to higher values.

To fit the TA and TO dispersions for $x = 0.8\%$ and $x = 1.5\%$, we used a mean-field solution of the Landau–Ginzburg–Devonshire (LGD) model including flexoelectric coupling [30, 39], shown as dotted lines in Fig. 2c,d. In this framework, as the TO mode softens and approaches the TA branch, the flexoelectric coupling f induces a softening of the TA mode that is maximal at a finite wavevector. When f approaches a critical value f_c , the TA branch develops a minimum that eventually reaches zero at $f = f_c$, signaling the onset of an incommensurate, spatially modulated phase. Figure 2e illustrates the evolution of both modes for different ratios

f/f_c and compare with the TA and TO dispersions for $x = 0.8\%$.

To limit the number of fitting parameters, we fixed the elastic constants to values obtained from ultrasound measurements [32] and considered only static flexoelectricity. Only three parameters were adjusted to reproduce the TA dispersion (see [31], Sec. D). Using $f \simeq 6 \text{ V}$, comparable to experimentally reported values [40], the model quantitatively reproduces both TO and TA dispersions for $x = 0.8\%$, corresponding to $f/f_c \simeq 0.8$. In contrast, it fails to capture the waterfall-like dispersion observed at $x = 1.5\%$, suggesting that a more sophisticated approach, including a q -dependent flexoelectric coefficient or self-consistent phonon approximation is required.

Contrary to the model proposed by [7], where ferroelectricity and modulated phase instabilities compete, we observe their simultaneous and cooperative presence. One identifiable source of this cooperation is the splitting of the TO mode below T_{AFD} [41]. The tetragonal distor-

tion splits the polar mode into A_{2u} and E_u branches, with the splitting proportional to the octahedral tilt angle φ [42, 43]. Ca doping increases φ [44], enhancing the splitting of the polar soft mode, which in turn favors the emergence of a modulated phase. Interestingly, we show that the TA softening begins once $T < T_{\text{AFD}}$, see Fig. 3b and c), providing further evidence that both the AFD distortion and the modulated phase cooperate.

These momentum-space instabilities point to multi-scale ferroelectric structures, such as the one illustrated on Fig. 4f). In highly polarizable $\text{Sr}_{1-x}\text{Ca}_x\text{TiO}_3$, local dipoles form around Ca atoms, breaking inversion symmetry [45, 46]. As the Ca concentration increases, these dipoles percolate into a macroscopic ferroelectric state [46, 47]. Our work reveals a second, larger length scale, $\ell_{\text{min}} \sim 10$ nm, associated with dynamically fluctuating domains. The coexistence of short-range ferroelectric regions and extended modulations demonstrates that the ground state is inherently multiscale, combining local ferroelectric order with a dynamically modulated lattice texture.

In conclusion, we show the quantum paraelectric regime of SrTiO_3 lies at the intersection of three intertwined lattice instabilities: ferroelectricity, AFD transition, and modulated phase. This finding is essential for understanding its unusual lattice properties, ranging from electric permittivity [19, 20, 48] and thermal conductivity [49] to low-frequency ultrasound [50] and light-induced phases [8, 37, 38, 51], and may also underline the

enhancement of superconductivity in ferroelectric superconductors [52–57]. Controlling this dynamical modulation via strain, electric fields, or carrier doping provides a promising route for engineering emergent ferroic behavior in quantum paraelectrics and their interfaces.

Acknowledgements

We thanks A. Bussmann-Holder, G.G Guzmán-Verri, P. Littlewood, A. N. Morozovska, E. Salje, A. Subedi and N. Spaldin for useful discussions. This work was supported by Jeunes Equipes de l’Institut de Physique du Collège de France and by a grant attributed by the Ile de France regional council. We acknowledge the European Synchrotron Radiation Facility for provision of beamtime under the proposal HC-5544. This work was also supported by Japan Society for the Promotion of Science (JSPS) KAKENHI Grant Numbers 23H01135 and 23K25832.

Data availability

INS data are available at <https://doi.ill.fr/10.5291/ILLDATA.701572>, <https://doi.ill.fr/10.5291/ILL-DATA.CRG-2926> and <https://doi.ill.fr/10.5291/ILLDATA.701606>. The rest of the data that support the findings of this study is available from the corresponding authors upon request.

[1] M. Seul and D. Andelman, Domain shapes and patterns: The phenomenology of modulated phases, *Science* **267**, 476 (1995), <https://www.science.org/doi/pdf/10.1126/science.267.5197.476>.

[2] E. Dagotto, Complexity in strongly correlated electronic systems, *Science* **309**, 257 (2005), <https://www.science.org/doi/pdf/10.1126/science.1107559>.

[3] G. C. Milward, M. J. Calderón, and P. B. Littlewood, Electronically soft phases in manganites, *Nature* **433**, 607 (2005).

[4] B. Keimer, S. A. Kivelson, M. R. Norman, S. Uchida, and J. Zaanen, From quantum matter to high-temperature superconductivity in copper oxides, *Nature* **518**, 179 (2015).

[5] M. P. Lilly, K. B. Cooper, J. P. Eisenstein, L. N. Pfeiffer, and K. W. West, Evidence for an anisotropic state of two-dimensional electrons in high landau levels, *Phys. Rev. Lett.* **82**, 394 (1999).

[6] B. Fauqué, P. Bourges, A. Subedi, K. Behnia, B. Bapteste, B. Roessli, T. Fennell, S. Raymond, and P. Steffens, Mesoscopic fluctuating domains in strontium titanate, *Phys. Rev. B* **106**, L140301 (2022).

[7] G. G. Guzmán-Verri, C. H. Liang, and P. B. Littlewood, Lamellar fluctuations melt ferroelectricity, *Phys. Rev. Lett.* **131**, 046801 (2023).

[8] G. Orenstein, V. Krapivin, Y. Huang, Z. Zhang, G. de la Peña Muñoz, R. A. Duncan, Q. Nguyen, J. Stanton, S. Teitelbaum, H. Yavas, T. Sato, M. C. Hoffmann, P. Kramer, J. Zhang, A. Cavalleri, R. Comin, M. P. M. Dean, A. S. Disa, M. Först, S. L. Johnson, M. Mitrano, A. M. Rappe, D. A. Reis, D. Zhu, K. A. Nelson, and M. Trigo, Observation of polarization density waves in SrTiO_3 , *Nature Physics* **10**.1038/s41567-025-02874-0 (2025).

[9] Y. Zhang, S. H. Sung, N. Agarwal, M. Gates, C. Li, P. Yu, R. Hovden, and I. E. Baggari, Nanoscale polar landscapes in quantum paraelectric SrTiO_3 (2025), arXiv:2509.24969 [cond-mat.mtrl-sci].

[10] D. Kaplan, P. A. Volkov, A. Chakraborty, Z. Zhuang, and P. Chandra, Tunable spatiotemporal orders in driven insulators, *Phys. Rev. Lett.* **134**, 066902 (2025).

[11] H. T. K. A. Müller, *Structural Phase Transitions I. (Topics in Current Physics)*, Berlin:Springer-Verlag, 1981).

[12] C. Collignon, X. Lin, C. W. Rischau, B. Fauqué, and K. Behnia, Metallicity and Superconductivity in Doped Strontium Titanate, *Annual Review of Condensed Matter Physics* **10**, 25 (2019).

[13] K. A. Müller and H. Burkard, SrTiO_3 : An intrinsic quantum paraelectric below 4 K, *Phys. Rev. B* **19**, 3593 (1979).

[14] T. Schneider, H. Beck, and E. Stoll, Quantum effects in an n -component vector model for structural phase tran-

sitions, *Phys. Rev. B* **13**, 1123 (1976).

[15] D. Shin, S. Latini, C. Schäfer, S. A. Sato, U. De Giovannini, H. Hübener, and A. Rubio, Quantum paraelectric phase of SrTiO_3 from first principles, *Phys. Rev. B* **104**, L060103 (2021).

[16] T. Esswein and N. A. Spaldin, Ferroelectric, quantum paraelectric or paraelectric? Calculating the evolution from BaTiO_3 to SrTiO_3 to KTaO_3 using a single-particle quantum-mechanical description of the ions (2021), arXiv:2112.11284 [cond-mat.mtrl-sci].

[17] K. A. Müller, W. Berlinger, and E. Tosatti, Indication for a novel phase in the quantum paraelectric regime of SrTiO_3 , *Zeitschrift für Physik B Condensed Matter* **84**, 277 (1991).

[18] A. Bussmann-Holder, H. Büttner, and A. R. Bishop, Polar-soft-mode-driven structural phase transition in SrTiO_3 , *Phys. Rev. Lett.* **99**, 167603 (2007).

[19] S. E. Rowley, L. J. Spalek, R. P. Smith, M. P. M. Dean, M. Itoh, J. F. Scott, G. G. Lonzarich, and S. S. Saxena, Ferroelectric quantum criticality, *Nature Physics* **10**, 367 (2014).

[20] M. J. Coak, C. R. S. Haines, C. Liu, S. E. Rowley, G. G. Lonzarich, and S. S. Saxena, Quantum critical phenomena in a compressible displacive ferroelectric, *Proceedings of the National Academy of Sciences* **117**, 12707 (2020), <https://www.pnas.org/content/117/23/12707.full.pdf>.

[21] Y. Yamada and G. Shirane, Neutron Scattering and Nature of the Soft Optical Phonon in SrTiO_3 , *Journal of the Physical Society of Japan* **26**, 396 (1969), <https://doi.org/10.1143/JPSJ.26.396>.

[22] R. Vacher, J. Pelous, B. Hennion, G. Coddens, E. Courtens, and K. A. Müller, Anomalies in the ta-phonon branches of SrTiO_3 in the quantum paraelectric regime, *Europhysics Letters* **17**, 45 (1992).

[23] E. Courtens, G. Coddens, B. Hennion, B. Hehlen, J. Pelous, and R. Vacher, Phonon anomalies in SrTiO_3 in the quantum paraelectric regime, *Physica Scripta* **T49B**, 430 (1993).

[24] E. V. Balashova, V. V. Lemanov, R. Kunze, G. Martin, and M. Weihnacht, Ultrasonic study on the tetragonal and muller phase in SrTiO_3 , *Ferroelectrics* **183**, 75 (1996), <https://doi.org/10.1080/00150199608224093>.

[25] B. Hehlen, Z. Kallassy, and E. Courtens, The high-frequency elastic constants of SrTiO_3 in the quantum paraelectric regime, *Ferroelectrics* **183**, 265 (1996), <https://doi.org/10.1080/00150199608224113>.

[26] B. Hehlen, L. Arzel, A. K. Tagantsev, E. Courtens, Y. Inaba, A. Yamanaka, and K. Inoue, Brillouin-scattering observation of the TA-TO coupling in SrTiO_3 , *Phys. Rev. B* **57**, R13989 (1998).

[27] X. He, D. Bansal, B. Winn, S. Chi, L. Boatner, and O. Delaire, Anharmonic Eigenvectors and Acoustic Phonon Disappearance in Quantum Paraelectric SrTiO_3 , *Phys. Rev. Lett.* **124**, 145901 (2020).

[28] B. S. de Lima, M. S. da Luz, F. S. Oliveira, L. M. S. Alves, C. A. M. dos Santos, F. Jomard, Y. Sidis, P. Bourges, S. Harms, C. P. Grams, J. Hemberger, X. Lin, B. Fauqué, and K. Behnia, Interplay between antiferrodistortive, ferroelectric, and superconducting instabilities in $\text{Sr}_{1-x}\text{Ca}_x\text{TiO}_3$ *Phys. Rev. B* **91**, 045108 (2015).

[29] J. G. Bednorz and K. A. Müller, $\text{Sr}_{1-x}\text{Ca}_x\text{TiO}_3$: An XY quantum ferroelectric with transition to randomness, *Phys. Rev. Lett.* **52**, 2289 (1984).

[30] A. N. Morozovska, M. D. Glinchuk, E. A. Eliseev, and Y. M. Vysotskii, Flexocoupling-induced soft acoustic modes and the spatially modulated phases in ferroelectrics, *Phys. Rev. B* **96**, 094111 (2017).

[31] See Supplemental Material for the presentation of the samples, the spectrometer configurations, the experimental fitting procedure and additional raw data [58].

[32] M. A. Carpenter, Elastic anomalies accompanying phase transitions in $(\text{Ca},\text{Sr})\text{TiO}_3$ perovskites: Part I. Landau theory and a calibration for SrTiO_3 , *American Mineralogist* **92**, 309 (2007), https://pubs.geoscienceworld.org/msa/ammin/article-pdf/92/2-3/309/3620965/9_2295Carpenter1.indd.pdf.

[33] P. M. Gehring, S.-E. Park, and G. Shirane, Soft phonon anomalies in the relaxor ferroelectric $\text{Pb}(\text{Zn}_{1/3}\text{Nb}_{2/3})_{0.92}\text{Ti}_{0.08}\text{O}_3$, *Phys. Rev. Lett.* **84**, 5216 (2000).

[34] P. M. Gehring, S. Wakimoto, Z.-G. Ye, and G. Shirane, Soft mode dynamics above and below the burns temperature in the relaxor $\text{Pb}(\text{Mg}_{1/3}\text{Nb}_{2/3})\text{O}_3$, *Phys. Rev. Lett.* **87**, 277601 (2001).

[35] J. Hlinka, S. Kamba, J. Petzelt, J. Kulda, C. A. Randall, and S. J. Zhang, Origin of the “waterfall” effect in phonon dispersion of relaxor perovskites, *Phys. Rev. Lett.* **91**, 107602 (2003).

[36] X. Li, T. Qiu, J. Zhang, E. Baldini, J. Lu, A. M. Rappe, and K. A. Nelson, Terahertz field induced ferroelectricity in quantum paraelectric SrTiO_3 , *Science* **364**, 1079 (2019), <https://www.science.org/doi/pdf/10.1126/science.aaw4913>.

[37] T. F. Nova, A. S. Disa, M. Fechner, and A. Cavalleri, Metastable ferroelectricity in optically strained SrTiO_3 , *Science* **364**, 1075 (2019), <https://www.science.org/doi/pdf/10.1126/science.aaw4911>.

[38] M. Fechner, M. Först, G. Orenstein, V. Krapivin, A. S. Disa, M. Buzzi, A. von Hoegen, G. de la Pena, Q. L. Nguyen, R. Mankowsky, M. Sander, H. Lemke, Y. Deng, M. Trigo, and A. Cavalleri, Quenched lattice fluctuations in optically driven SrTiO_3 , *Nature Materials* **23**, 363 (2024).

[39] A. N. Morozovska, E. A. Eliseev, C. M. Scherbakov, and Y. M. Vysotskii, Influence of elastic strain gradient on the upper limit of flexocoupling strength, spatially modulated phases, and soft phonon dispersion in ferroics, *Phys. Rev. B* **94**, 174112 (2016).

[40] C. A. Mizzi, B. Guo, and L. D. Marks, Experimental determination of flexoelectric coefficients in SrTiO_3 , KTaO_3 , TiO_2 , and YAlO_3 single crystals, *Phys. Rev. Mater.* **6**, 055005 (2022).

[41] H. Uwe and T. Sakudo, Stress-induced ferroelectricity and soft phonon modes in SrTiO_3 , *Phys. Rev. B* **13**, 271 (1976).

[42] A. Yamanaka, M. Kataoka, Y. Inaba, K. Inoue, B. Hehlen, and E. Courtens, Evidence for competing orderings in strontium titanate from hyper-Raman scattering spectroscopy, *Europhysics Letters (EPL)* **50**, 688 (2000).

[43] B. Hehlen, A. Al-Zein, C. Bogicevic, P. Gemeiner, and J.-M. Kiat, Soft-mode dynamics in micrograin and nanograin ceramics of strontium titanate observed by hyper-raman scattering, *Phys. Rev. B* **87**, 014303 (2013).

[44] G. Geneste and J.-M. Kiat, Ground state of ca-doped strontium titanate: Ferroelectricity versus polar nanoregions, *Phys. Rev. B* **77**, 174101 (2008).

- [45] B. E. Vugmeister and M. D. Glinchuk, Dipole glass and ferroelectricity in random-site electric dipole systems, *Rev. Mod. Phys.* **62**, 993 (1990).
- [46] G. A. Samara, The relaxational properties of compositionally disordered ABO_3 perovskites, *Journal of Physics: Condensed Matter* **15**, R367 (2003).
- [47] U. Bianchi, J. Dec, W. Kleemann, and J. G. Bednorz, Cluster and domain-state dynamics of ferroelectric $\text{Sr}_{1-x}\text{Ca}_x\text{TiO}_3$ ($x=0.007$), *Phys. Rev. B* **51**, 8737 (1995).
- [48] J. Li, Y. Lee, Y. Choi, J.-W. Kim, P. Thompson, K. J. Crust, R. Xu, H. Y. Hwang, P. J. Ryan, and W.-S. Lee, The classical-to-quantum crossover in the strain-induced ferroelectric transition in SrTiO_3 membranes, *Nature Communications* **16**, 4445 (2025).
- [49] V. Martelli, J. L. Jiménez, M. Continentino, E. Baggio-Saitovitch, and K. Behnia, Thermal Transport and Phonon Hydrodynamics in Strontium Titanate, *Phys. Rev. Lett.* **120**, 125901 (2018).
- [50] S. Kustov, I. Liubimova, and E. K. H. Salje, Domain Dynamics in Quantum-Paraelectric SrTiO_3 , *Phys. Rev. Lett.* **124**, 016801 (2020).
- [51] X. Li, T. Qiu, J. Zhang, E. Baldini, J. Lu, A. M. Rappe, and K. A. Nelson, Terahertz field induced ferroelectricity in quantum paraelectric SrTiO_3 , *Science* **364**, 1079 (2019).
- [52] C. W. Rischau, X. Lin, C. P. Grams, D. Finck, S. Harms, J. Engelmayr, T. Lorenz, Y. Gallais, B. Fauqué, J. Hemberger, and K. Behnia, A ferroelectric quantum phase transition inside the superconducting dome of $\text{Sr}_{1-x}\text{Ca}_x\text{TiO}_{3-d}$, *Nature Physics* **13**, 643 (2017).
- [53] Y. Tomioka, N. Shirakawa, K. Shibuya, and I. H. Inoue, Enhanced superconductivity close to a non-magnetic quantum critical point in electron-doped strontium titanate, *Nature Communications* **10**, 738 (2019).
- [54] K. Ahadi, L. Galletti, Y. Li, S. Salmani-Rezaie, W. Wu, and S. Stemmer, Enhancing superconductivity in SrTiO_3 films with strain, *Science Advances* **5**, eaaw0120 (2019), <https://www.science.org/doi/pdf/10.1126/sciadv.aaw0120>.
- [55] C. W. Rischau, D. Pulmannová, G. W. Scheerer, A. Stucky, E. Giannini, and D. van der Marel, Isotope tuning of the superconducting dome of strontium titanate, *Phys. Rev. Research* **4**, 013019 (2022).
- [56] Y. Tomioka, N. Shirakawa, and I. H. Inoue, Superconductivity enhancement in polar metal regions of $\text{Sr}_{0.95}\text{Ba}_{0.05}\text{TiO}_3$ and $\text{Sr}_{0.985}\text{Ca}_{0.015}\text{TiO}_3$ revealed by systematic Nb doping, *npj Quantum Materials* **7**, 111 (2022).
- [57] S. Zhang, X. Xu, and R. J. Cava, Induced ferroelectricity and enhanced superconductivity through b-site doped $\text{SrTi}_{1-x}\text{Zr}_x\text{O}_3$, *Phys. Rev. B* **111**, 054522 (2025).
- [58] T. Weber, Update 2.0 to Takin: An open-source software for experiment planning, visualisation, and data analysis, *SoftwareX* **14**, 100667 (2021).